



NRC Publications Archive Archives des publications du CNRC

Two-pulse and stimulated nuclear-quadrupole-resonance echoes in YAlO₃:Pr³⁺ Erickson, L. E.

This publication could be one of several versions: author's original, accepted manuscript or the publisher's version. /
La version de cette publication peut être l'une des suivantes : la version prépublication de l'auteur, la version
acceptée du manuscrit ou la version de l'éditeur.

For the publisher's version, please access the DOI link below. / Pour consulter la version de l'éditeur, utilisez le lien
DOI ci-dessous.

Publisher's version / Version de l'éditeur:

<https://doi.org/10.1103/PhysRevB.43.12723>

Physical Review B, 43, 16, pp. 12723-12728, 1991-06

NRC Publications Record / Notice d'Archives des publications de CNRC:

<https://nrc-publications.canada.ca/eng/view/object/?id=e8953eca-7e57-420d-9498-9f280afc21ee>

<https://publications-cnrc.canada.ca/fra/voir/objet/?id=e8953eca-7e57-420d-9498-9f280afc21ee>

Access and use of this website and the material on it are subject to the Terms and Conditions set forth at

<https://nrc-publications.canada.ca/eng/copyright>

READ THESE TERMS AND CONDITIONS CAREFULLY BEFORE USING THIS WEBSITE.

L'accès à ce site Web et l'utilisation de son contenu sont assujettis aux conditions présentées dans le site

<https://publications-cnrc.canada.ca/fra/droits>

LISEZ CES CONDITIONS ATTENTIVEMENT AVANT D'UTILISER CE SITE WEB.

Questions? Contact the NRC Publications Archive team at

PublicationsArchive-ArchivesPublications@nrc-cnrc.gc.ca. If you wish to email the authors directly, please see the
first page of the publication for their contact information.

Vous avez des questions? Nous pouvons vous aider. Pour communiquer directement avec un auteur, consultez la
première page de la revue dans laquelle son article a été publié afin de trouver ses coordonnées. Si vous n'arrivez
pas à les repérer, communiquez avec nous à PublicationsArchive-ArchivesPublications@nrc-cnrc.gc.ca.



Two-pulse and stimulated nuclear-quadrupole-resonance echoes in $\text{YAlO}_3:\text{Pr}^{3+}$

L. E. Erickson

National Research Council, Ottawa, Ontario, Canada K1A 0R8

(Received 17 December 1990; revised manuscript received 4 February 1991)

The dephasing of trivalent praseodymium dilute in yttrium aluminum oxide (YAlO_3) in the ground electronic state 3H_4 state is evaluated using an optically detected method, to measure two-rf-pulse- and three-rf-pulse-stimulated nuclear quadrupole echoes. The magnitude of the echo is obtained by detecting the weak Raman optical field generated by the interaction of the magnetic moment of the echo and a light beam resonant with the $^3H_4(0\text{ cm}^{-1})$ to $^1D_2(16\,374\text{ cm}^{-1})$ optical transition. This same light beam is used as an optical pump (37-ms duration) prior the rf-pulse sequence to increase the population difference of the hyperfine energy levels, thereby improving the echo signal. The light is turned off 9 ms before the rf-pulse sequence and remains off until the echo to avoid optical-pumping effects on the measured nuclear-quadrupole-resonance (NQR) echo lifetime. The dephasing time T_2 from two-pulse nuclear-quadrupole-echo measurement is found to be $366 \pm 29\ \mu\text{s}$. Three-pulse-stimulated echoes show a fast decay at short times, followed by a slower (240 ms) decay. The Hu-Hartmann uncorrelated-sudden-jump model was fitted to the data. For the two-pulse echo, the best approximation to the data is obtained using a fluctuating field amplitude $\Delta\omega_{1/2} = 7000\text{ s}^{-1}$, and the fluctuation rate $W = 2100\text{ s}^{-1}$. In contrast to this, the three-pulse echo data, measured with a much smaller separation of the first two pulses τ , shows an approximate fit using $\Delta\omega_{1/2} \approx 60\,000\text{ s}^{-1}$ ($\tau < 40\ \mu\text{s}$) and $W = 12\text{ s}^{-1}$ for data plotted versus the separation between the second and third rf pulses T for several values of the separation of the first two pulses τ , and $\Delta\omega_{1/2} = 125\,000\text{ s}^{-1}$ and $W = 20\text{ s}^{-1}$ for data at three fixed values of T , plotted versus τ . The apparent discrepancy between the two-pulse and the three-pulse fits is attributed to two different dephasing host Al nuclei. The fluctuating fields due to bulk Al are effective in dephasing the Pr moment for $\tau \geq T_2$, and the frozen-core Al, which surround the Pr^{3+} ion, produce a much larger effective field that fluctuates much more slowly, are the dephasing agent for $\tau \ll T_2$.

INTRODUCTION

The host-guest system $\text{YAlO}_3:\text{Pr}^{3+}$ has attracted considerable recent interest as a spectroscopic material^{1,2} and a laser host.³ In particular, for optical storage, it is important to know the mechanisms involved in the relaxation of optical coherence (optical dephasing time). Any phase interruption of the optical terminal levels interrupts the optical coherence. This includes the dephasing within hyperfine sublevels of both the ground and excited states, as well as the radiative decay of the optically excited state. Hyperfine sublevel dephasing is caused by spin-lattice relaxation of the impurity ion studied (T_1), and by dipolar interactions (T_2) with neighboring nuclear moments either of the host (Al, Y) or by other impurity (Pr^{3+}) ions. One reason for choosing the YAlO_3 as a host is that the relatively small nuclear dipole fields ($\approx 1\text{ G}$) at the impurity site produce a narrow inhomogeneous linewidth of the impurity ion. The optical dephasing time in this material was measured by Macfarlane *et al.*⁴ to be $78\ \mu\text{s}$ in the presence of a static magnetic field, slightly less than $\frac{1}{2}$ of the excited-state lifetime. This would indicate that the contribution of the excited-state lifetime to the optical dephasing time is about one-quarter of the observed rate. In this paper, measurements of two-pulse nuclear-quadrupole-resonance (NQR) echo decay and three-pulse NQR (stimulated) echo decay

are reported, and the dephasing time T_2 for two-pulse echoes is obtained for the 3H_4 ground state of $\text{YAlO}_3:\text{Pr}^{3+}$. The hyperfine sublevel population decay rate T_1 is obtained from the three-pulse echo data. These measurements indicate that the stimulated echo decays faster immediately after the coherence is prepared by the two $\pi/2$ pulses than at later times. This is normally considered due to spectral diffusion due to changing local fields as the host nuclear spins flip causing some of the prepared impurity spins to change resonant frequencies so that they cannot be refocused by the third $\pi/2$ pulse. The Hu-Hartmann uncorrelated-sudden-jump model⁵ is applied to the data. The fit of the theory to the data show two distinctly different regimes. The two-pulse echo fit shows rapid fluctuations with a small fluctuating field amplitude. The three-pulse echo amplitude shows only a very slow fluctuation rate, but with a large fluctuating field amplitude, which increases slightly with the separation of the first two rf pulses. These two regimes represent dephasing by two different sets of Al host nuclei, one described as the bulk, and the other in the frozen core surrounding a Pr^{3+} ion.

EXPERIMENT

Measurements of two-pulse- and three-pulse-stimulated NQR echo decay in this dilute material were made using

Raman heterodyne optical detection.⁶ This three-wave mixing technique, in which a *sample light* field interacts with the *magnetization* in the sample introduced by the rf pulses to produce another collinear optical field (the Raman heterodyne signal) at the difference frequency, is shown in Fig. 1. This second optical field is detected by mixing it with the first on a photodiode. This signal at the NQR frequency is demodulated by mixing it with the rf driving the pulse programmer. The experiment is summarized in Fig. 2. The top line shows the time pattern for the light. A 37-ms pulse of narrowband light resonant with the $^1D_2\text{-}^3H_4$ ($16\,374.7\text{ cm}^{-1}$) transition, is used to create a nonequilibrium population distribution in the hyperfine sublevels of the ground state. This light source is turned on again for $24\ \mu\text{s}$ centered at the echo. Keeping the light off during the pulse train avoids any optical pumping effects on the echo decay. The bottom line of Fig. 2 specifically shows the rf-pulse pattern for the stimulated echo. A two-pulse echo is obtained by setting $T=0$. The $\pi/2$ rf pulses are 80 rf cycles in duration. The middle line of Fig. 2 shows the echo signal. The $\text{YAlO}_3\text{:Pr}^{3+}$ (0.1 at %) is placed into a delay line rf coil⁷ in a cryostat near 5.5 K. The frequency-stabilized (± 0.5 MHz) single-frequency cw dye laser light (≈ 2 mW) is gated by an acousto-optic (A/O) modulator (1000:1 contrast) and focused onto the sample by an 80-cm-focal-length lens. The transmitted light impinges on the photodiode of an optical receiver. The pulse sequence is repeated at 11-sec intervals, which is long enough to allow the complete relaxation of the ground state. Each point on a decay curve is derived from an average of 32 pulse sequences. A typical decay for a two-pulse echo sequence

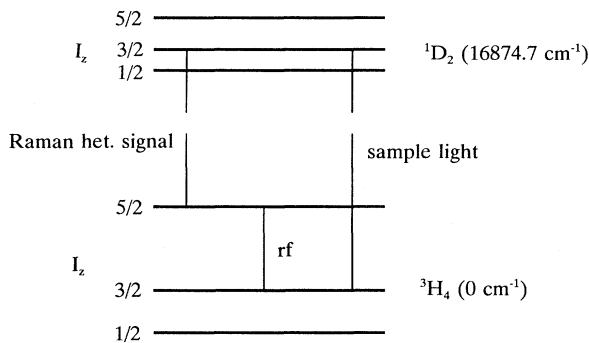


FIG. 1. The Raman heterodyne detection of NQR echoes in Pr^{3+} dilute in YAlO_3 is described using a diagram of the hyperfine sublevels. The sample light field, Raman heterodyne signal and the rf-pulse fields are indicated. The Raman heterodyne signal is generated by the sample light field and the magnetization of the praseodymium produced by the rf pulses. Only one of six possible optical channels is shown. Because the optical inhomogeneous broadening greatly exceeds the hyperfine splittings, different Pr^{3+} ions are resonant with the optical field for other combinations of ground and excited hyperfine levels. The rf selects only the $I_z = \frac{3}{2}$ to $I_z = \frac{5}{2}$ hyperfine transition in the ground state. For simplicity, the small magnetic-field splitting of the hyperfine levels is ignored.

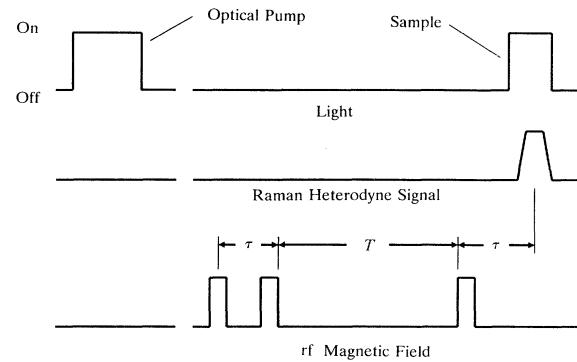


FIG. 2. The pulse sequences used in the experiment. The upper line shows the *on* periods for the dye laser light. Each echo measurement begins with a 37-ms optical pump period after which the light beam is turned off. The light is turned on again for a $24\text{-}\mu\text{s}$ period surrounding the echo. The lower curve displays the rf-pulse pattern. 9 ms after the end of the optical pump, the rf-pulse sequence begins. For a two-pulse echo, $T=0$. The center line shows the Raman heterodyne signal. Only the echo magnetization is observed; the free induction decay immediately after the rf pulse is not observed because the sample light is off. The entire process is repeated at 11-sec intervals so that 32 echo amplitudes may be averaged.

is shown in Fig. 3. When the echo decay is fitted to a simple exponential $\exp(2\tau/T_2)$, a mean value for $T_2 = 366 \pm 29\ \mu\text{s}$ was obtained from six similar decay curves.

The three-pulse stimulated echo measurements were more complex in that we have two variables, the separation of the first two $\pi/2$ rf pulses τ , and the time between the second and third $\pi/2$ pulse T . A series of measurements versus T for fixed τ are shown in Fig. 4. For $2\tau \approx T_2$, the stimulated echo decay is rapid, while for very small values, a rapid initial decay is observed followed by

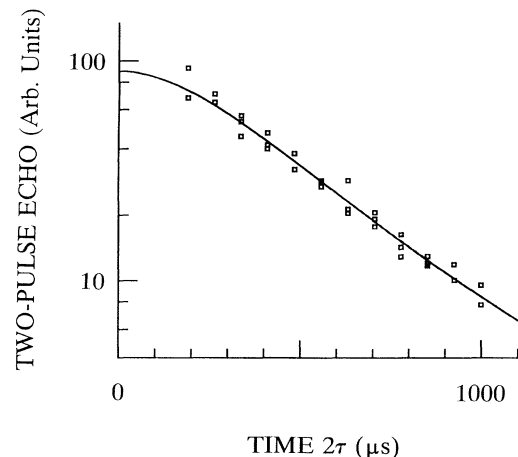


FIG. 3. Two-pulse NQR echo amplitude vs 2τ , the time from the middle of the first rf pulse until the middle of the echo. The solid line is derived from the exact Hu-Hartmann model using $\Delta\omega_{1/2} = 7000\text{ s}^{-1}$ and $W = 2100\text{ s}^{-1}$.

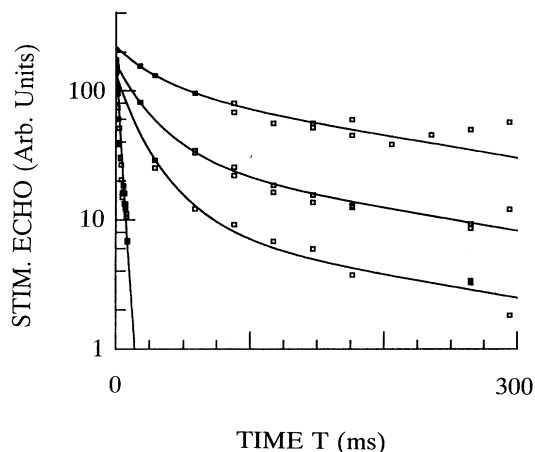


FIG. 4. Three-pulse (stimulated) NQR echo amplitude vs T , the time between the end of the second $\pi/2$ pulse and the beginning of the third $\pi/2$ pulse, for fixed values of $\tau=19, 29, 38$, and $151 \mu\text{s}$ (from top to bottom). The solid lines are derived from the Hu-Hartmann model using $W=12 \text{ s}^{-1}$, and $\Delta\omega_{1/2}=40\,000, 60\,000, 70\,000$, and $120\,000 \text{ s}^{-1}$. A spin-lattice decay term with $T_1=0.24 \text{ s}$ is included. The spin-lattice term is responsible for the nonzero slope of the solid line for large T .

a slow decay significantly longer than that observed in the multipulse spin-locking experiments.⁸ More detail for small τ is given in Fig. 5, where sections of Fig. 4 for fixed values of T equal to 3.7, 14.7, and 59 ms are given. Another line could be added for $T=0$, which would be an extrapolation of the data of Fig. 3. These curves clearly demonstrate the necessity of the preparation time τ being short compared to T_2 for long-lived stimulated echoes. The long slow decay time was measured to be

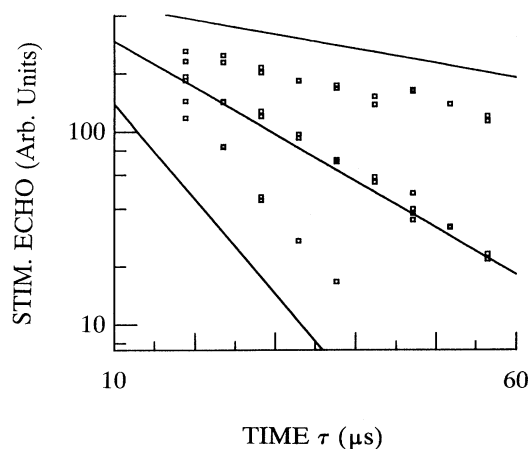


FIG. 5. Three-pulse NQR echo amplitude vs τ for three values of $T=3.7, 14.7$, and 59 ms (from top to bottom). The solid lines are derived from the Hu-Hartmann model using $\Delta\omega_{1/2}=120\,000 \text{ s}^{-1}$, $W=20 \text{ s}^{-1}$, and $T_1=0.24 \text{ s}$. The spin-lattice term reduces the amplitude of the echo for larger T but has no practical effect on the slope of these curves.

240 ms for $\tau=29 \mu\text{s}$ and a sample temperature of $5.48\pm 0.08 \text{ K}$. This is the second curve from the top of Fig. 4. Because the spin-lattice relaxation rate changes rapidly with temperature, these data were taken with a constant temperature. The deviation for each of these runs was less than $\pm 0.1 \text{ K}$. To avoid effects of slowly changing sample temperatures and detection light power, the points were taken in random order rather than by stepped increases. Experimental points which lay outside of the temperature and power limits were deleted.

DISCUSSION

It is instructive to compare these two-pulse echo results with previous measurements in $\text{LaF}_3:\text{Pr}^{3+}$. The nuclear spin dephasing time for Pr^{3+} has been measured in LaF_3 (Ref. 9) as $T_2=17 \mu\text{s}$ in zero external magnetic field, and by Wong *et al.*¹⁰ ($29 \mu\text{s}$) in a 30-G external field and by the author¹¹ ($37 \mu\text{s}$) in an 80-G external field. The dephasing is thought to be caused by fluctuations in the local fields at the Pr (A -spin) nucleus by the host (B -spin) nuclear moments. For LaF_3 , the F (B -spin) moment is large and nearby the Pr (A -spin) nucleus. A relative measure of the strength of this dipolar field is given by the zero-static magnetic-field inhomogeneous NQR linewidth of $\Delta\nu=180 \text{ kHz}$ (FWHM). This compares to $\Delta\nu=56 \text{ kHz}$ (FWHM) for Pr^{3+} in YAlO_3 .¹² It is, therefore, somewhat surprising that the measured T_2 is ten times longer for the YAlO_3 host than for the LaF_3 host crystal. Several things enter into the relationship between the magnetic-field fluctuations and the dephasing time. The phase interruptions are caused by changes in the local magnetic field at each Pr^{3+} ion which change its magnetic resonance frequency (spectral diffusion). The rate of change of the environment W is the flip-flop rate of neighboring B spin nuclear moments (Al or F). The magnitude of the change is large for a nearest-neighbor spin flip but small for a more distant spin rendering them less effective in interrupting the phase of the Pr nucleus. However, these more distant B spins are coupled strongly to the bulk Al nuclei resulting in rapid mutual spin flips, whereas the nearest neighbors (frozen core) are somewhat isolated because their Larmor frequencies are displaced from the bulk by the weak (Van Vleck) paramagnetic center. Measurements of the F T_2 in LaF_3 (Ref. 13) ($16 \mu\text{s}$) give an indication of their bulk rates. Unfortunately, the measurements¹⁴ of Al NMR and NQR that have been made of YAlO_3 do not include dynamic data.

Since the bulk B -spin nuclei are coupled to one another, a T_2 spectral diffusion model would best describe the physical processes taking place in this abundant B -spin situation. Unfortunately, a T_2 model, in closed form, is not currently available. Therefore, the Hu-Hartmann spectral-diffusion model will be used to fit these experiments. The effect of the coupling will be to reduce the fluctuating field amplitudes seen by the A spin and to increase the flipping rate W . The nearest-neighbor B spins are, however, uncoupled from the bulk so the T_1 hypotheses of the model are more closely followed in this system. In their paper on the measurement of two-pulse echoes of Pr^{3+} in LaF_3 , Shelby *et al.*⁹ obtained good

agreement between their zero-static magnetic-field echo data and the uncorrelated sudden jump model of Hu and Hartmann⁵ by using a fluctuating field amplitude $\Delta\omega_{1/2}=50\,000\text{ s}^{-1}$, significantly smaller than the inhomogeneous linewidth, and a fluctuation rate $W=59\,000\text{ s}^{-1}$ equal to the inverse of the measured dephasing rate $T_2=17\text{ }\mu\text{s}$ of the bulk F.¹⁵ The exact expression for the two-pulse echo is given by Hu and Hartmann as

$$E(2\tau)=\exp[-2\Delta\omega_{1/2}\tau K(2W\tau)], \quad (1)$$

where

$$\Delta\omega_{1/2}=\frac{16\pi^2}{9\sqrt{3}}n\frac{\mu_A\mu_B}{h/2\pi} \quad (2)$$

gives the static (inhomogeneous) dipolar width (HWHM) of the material due to the field of the host (B) spins acting on the guest (A) ion. n is the density of B spins, μ_A and μ_B are the nuclear moments of the A and B spins, respectively. (An estimate of this quantity may be derived from the experimentally observed NQR linewidths as mentioned in the preceding paragraph.) The function $K(z)$ is given by Hu and Hartmann in both graphical and tabular form. The solid line on Fig. 3 is derived from Eq. (1) using $\Delta\omega_{1/2}=7000\text{ s}^{-1}$ and $W=2100\text{ s}^{-1}$. The ratio $R=2W/\Delta\omega_{1/2}$ determines the shape of the decay. The best fit is obtained for this ratio. For larger values of R , the slope decreases at long times, whereas for small values of R , the two-pulse echo shows little decay at short times ($\Delta\omega_{1/2}\tau < 1$), but the decay increases to a maximum greater than T_2 at intermediate times, and finally settles to a τ^2 rate at long times. Hu and Hartmann [their Eq. (5.14)] also give the (lower) limiting echo amplitude versus the time τ between the $\pi/2$ and π pulses as

$$E_{\text{limit}}(2\tau)=\exp(-\pi^{-1/3}\Delta\omega_{1/2}\tau). \quad (3)$$

Equation 3 describes the echo decay for the first four or so time constants when the fluctuation rate $W\approx\Delta\omega_{1/2}/2$. Applying this limiting case to the two-pulse echo decay measurement of Fig. 3, one obtains

$$\Delta\omega_{1/2}=2(\pi^{1/3}/366\text{ }\mu\text{s})=8004\text{ s}^{-1}.$$

The straight line decay implies that the fluctuation rate $W\approx\Delta\omega_{1/2}/2$ because values departing significantly from this value show nonexponential decay behavior over the amplitude range of the measurement. (See Fig. 7 of Hu and Hartmann, Ref. 5.) The limiting case is a good approximation to the exact case for this situation.

This theory assumes that the A and B spins each have nuclear spin $I=\frac{1}{2}$ which do not interact with themselves (a T_1 model). For our A spins, $I=\frac{5}{2}$, but only the $I_z=\frac{3}{2}$ to $\frac{5}{2}$ transition is resonant with the rf magnetic field, so the usual spin Hamiltonian treatment of pseudospin $I=\frac{1}{2}$ may be used. In this approximation, the spin- I gyromagnetic ratio γ_A is used for the pseudospin $I'=\frac{1}{2}$ together with a modified magnetic field $H'=-\omega_{\text{r}}/\gamma_A$.¹⁶ Thus, one may calculate the dephasing time T_2 relative to LaF₃ using the γ_A ratio for the Pr³⁺ ions in LaF₃ and YAlO₃. A difficulty arises with the B spins which have spin $I=\frac{1}{2}$ for F in LaF₃ and $I=\frac{5}{2}$ for Al in YAlO₃. Since the model

calculates the field jumps at the A -spin site due to the flipping B spins, and each of these jumps is proportional to $\gamma_B\Delta I$, where $\Delta I=1$, the ratio of the two-pulse echo lifetimes of LaF₃ and YAlO₃ is approximately given by the ratio of the density n of the B spins and their gyromagnetic ratios γ_B . These are 5.5×10^{22} and $1.9\times 10^{22}\text{ cm}^{-3}$ and 4.09 and 1.11 kHz/G for F in LaF₃ and Al in YAlO₃ respectively. This gives a ratio of T_2 equal to 10.4 very close to the observed values 9.9. Equation 2 ignores the (enhanced) magnetic anisotropy present for the Pr³⁺ in these materials. The mean gyromagnetic ratios γ_A are 5.9 and 6.0 kHz/G for the two hosts.^{17,18} With the anisotropy, the ratio of T_2 is unchanged. It is clear that the long observed T_2 for this material is not totally unexpected, but the lack of an $I>\frac{1}{2}$ theory limits the applicability of the Hu-Hartmann two-pulse echo theory in this case of $I=\frac{5}{2}$ B spins.

Even with this nuclear spin limitation, an attempt is made to fit the stimulated NQR echo data. To be consistent, it must fit with the same parameters W and $\Delta\omega_{1/2}$ as for the T_2 decay. This three-pulse echo decay may be described as product of the two-pulse decay of Eq. (1) and a three-pulse decay term. The stimulated echo was given by Hu and Hartmann as

$$E_s(2\tau, T)=\exp[-2\Delta\omega_{1/2}\tau K(2W\tau)] \\ \times \exp\{-\Delta\omega_{1/2}\tau[G(2W\tau)-K(2W\tau)] \\ \times (1-e^{-2WT})\}. \quad (4)$$

The first exponential is the two-pulse echo decay [Eq. (1)], and the second term indicates the effect on the echo amplitude of splitting the π pulse into two parts separated by a time T . The functions $G(z)$ and $K(z)$, given by Hu and Hartmann (their Fig. 5 and Table I), never exceed unity and their difference is $1-z$ for low z and tends to $(1/2\pi)^{1/2}z^{-3/2}$ for large z . $K(z)\approx z/2$ for small z , reaches a maximum of 0.340 at $z=2.5$ and approaches $(2/\pi z)^{1/2}$ for large z . Using the parameters obtained from the two-pulse fit, the calculated stimulated echo decay only shows a small change in amplitude [$\approx \exp(-7000\tau)$] from the $T=0$ value to the $T=300\text{-ms}$ value, but with a rapid decay rate W . For $\tau=30\text{ }\mu\text{s}$, the calculated stimulated echo drops quickly ($500\text{ }\mu\text{s}$) to its final value, after which no further dephasing results. This is shown in Fig. 6 by the top curve labeled bulk. However, the experimental points are fitted by using much larger fluctuation amplitudes $\Delta\omega_{1/2}$ and much smaller fluctuation rates W . Because the stimulated echo measurement for $\tau=0$ is just the saturation recovery measurement of T_1 (a π pulse followed at time T by a $\pi/2$ pulse), the stimulated echo for $\tau=0$ should decay at this T_1 rate rather than being independent of T , as predicted by Eq. (4). With a spin-lattice decay term added to Eq. (4), the solid lines of Fig. 4 were obtained from Eq. (4) using $T_1=0.24\text{ s}$, $W=12$, $\Delta\omega_{1/2}=40\,000, 60\,000, 70\,000,$ and $120\,000\text{ s}^{-1}$ for $\tau=19, 28, 39,$ and $151\text{ }\mu\text{s}$. The $\Delta\omega_{1/2}\approx 100\,000-1.14/\tau\text{ s}^{-1}$ for $\tau\leq 40\text{ }\mu\text{s}$. The fit for the $\tau=29\text{-}\mu\text{s}$ curve of Fig. 4 is shown in Fig. 6 (without the spin-lattice term). The apparent weak dependence of

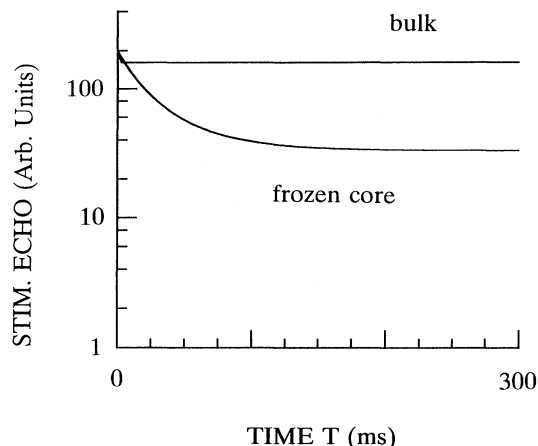


FIG. 6. Calculated three-pulse echo decay for frozen-core Al dephasing ($\Delta\omega_{1/2}=60\,000\text{ s}^{-1}$, $W=12\text{ s}^{-1}$) and for bulk Al dephasing ($\Delta\omega_{1/2}=7\,000\text{ s}^{-1}$, $W=2\,100\text{ s}^{-1}$) with $\tau=29\text{ }\mu\text{s}$. This demonstrates that the observed long-term dephasing is caused by the frozen-core Al nuclei. The spin-lattice term is omitted for this calculation.

$\Delta\omega_{1/2}$ on τ is not understood. Perhaps it is an indication of an interference because the rf pulse length $T_p=6\text{ }\mu\text{s}$ is not very small compared to the pulse separation τ .

The solid lines on Fig. 5 were also obtained using the Hu-Hartmann model, but using $T_1=0.25\text{ s}$, $W=20\text{ s}^{-1}$, and $\Delta\omega_{1/2}=125\,000\text{ s}^{-1}$. The lines match the slope of the experimental points, but not the amplitude. The model would predict that a larger amplitude change should occur for a given change in T . This is consistent with the fits for Fig. 4, where smaller values of $\Delta\omega_{1/2}$ are obtained from the fit. No attempt was made to include the functional dependence $\Delta\omega_{1/2}(\tau)$ obtained from the fit of Fig. 4.

The apparent discrepancy between the fits of Figs. 3 and 4 may be explained by the combination of two relaxation processes working in parallel. The frozen-core model proposed by Bloembergen,¹⁹ separates the host spins into two classes, those of the bulk unperturbed by any impurity moments and the others. The first class all have the same resonant frequencies and therefore engage in rapid mutual spin flips. The other host nuclei are detuned by the impurity moment so they do not engage in these rapid mutual spin flips—thus, the name frozen. The Hu-Hartmann model gives a description of the three-pulse echo which is internally consistent with the measured inhomogeneous broadening of the Pr^{3+} NQR resonance. [In an 80-G magnetic field, $\Delta\omega_{\text{NQR}}=88\,000\text{ s}^{-1}$ (HWHM)].²⁰ This large width is due to the nearest-neighbor Al nuclear moments (frozen core).¹⁰ The slow fluctuation rate $W=12\text{ s}^{-1}$ is attributed to these Al, which flip slowly (T_1 ?) because they are not coupled to the bulk Al, rather than to a Pr-Pr interaction. The Pr^{3+} ion is a Van Vleck paramagnet. In zero field, it has no *electronic* dipole moment. At 80 G there is a very small induced *electronic* dipole moment, too small to give a paramagnetic relaxation at these concentrations.²¹ In ad-

dition, this slow fluctuation rate does not match the measured Pr^{3+} spin-lattice relaxation rate $T_1=0.24\text{ s}^{-1}$. The NMR measurements of Al in YAlO_3 do not include any T_1, T_2 information, so no direct comparison can be made of the fluctuation rates W , obtained from fitting the Hu-Hartmann model to the two- and three-pulse data and the dynamics of the Al produced local magnetic fields. The two-pulse echo fit using the Hu-Hartmann model indicate that, for $\tau \geq T_2$, the fluctuating fields $\Delta\omega_{1/2}$ are much smaller [e.g., from distant (bulk) B spins] and their fluctuation rates W are much much faster (perhaps at the T_2 rate of the bulk Al nuclei) than those dephasing the three-pulse echo. If one calculates the two-pulse echo amplitude using the parameters which fit the three-pulse echo, one finds that these fluctuating fields are much less effective than those rapidly changing bulk Al fields. This is shown in the top curve of Fig. 7. This case is fortuitous because the frozen core causes only a small fraction of the dephasing of Fig. 3 whereas the bulk Al are totally ineffective in dephasing the stimulated echo. This explanation is consistent with the previous two-pulse $\text{LaF}_3:\text{Pr}^{3+}$ work of Shelby⁹ where they concluded that the bulk F were responsible for the two-pulse dephasing. They postulated that the frozen core was essentially static. The direct Al two-pulse measurements of Szabo *et al.*²² on ruby ($\text{Al}_2\text{O}_3:\text{Cr}^{3+}$) and these three-pulse measurements confirm such a postulate, but show that the core is not quite frozen. The results of this paper would appear to remove Al as a cause of the rapid photon echo dephasing rate observed by Macfarlane.⁴

The NQR line is inhomogeneously broadened [$\Delta\nu_{\text{NQR static}} \approx 28\text{ kHz}$ (FWHM) in 80-G magnetic field] and has a dynamic width $1/\pi T_2=870\text{ Hz}$. The $T_p=6\text{ }\mu\text{s}$ ($1/\pi T_p=53\text{ kHz}$) rf pulses used are nonselective, so the entire NQR line is excited and no spectral diffusion would normally be expected. But, in this optically detected experiment, there is an optical selection process whereby a packet of spins within the very much broader

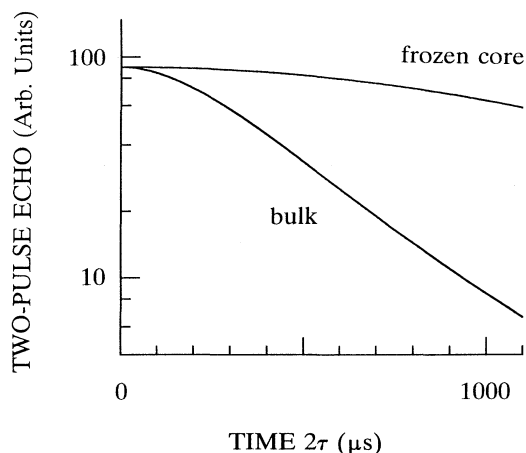


FIG. 7. Calculated two-pulse echo decay for frozen-core Al dephasing ($\Delta\omega_{1/2}=60\,000\text{ s}^{-1}$, $W=12\text{ s}^{-1}$) and for bulk Al dephasing ($\Delta\omega_{1/2}=7\,000\text{ s}^{-1}$, $W=2\,100\text{ s}^{-1}$). This demonstrates that the observed dephasing is caused by the bulk Al nuclei.

optical line is optically pumped, producing a nonequilibrium distribution of populations only for this group of optically selected nuclear spins. There is little correlation between the inhomogeneous optical broadening and inhomogeneous nuclear broadening so the optical pumping does not introduce NQR selectivity. But when B -spin flips occur, the optically pumped A spins are exchanged for nonoptically pumped A spins resulting in a loss of nuclear polarization in the measured A -spin packet. Therefore, the uncorrelated sudden jump model of the Hu-Hartmann model should apply to these measurements.

CONCLUSION

Two-pulse and stimulated NQR echoes have been measured from Pr^{3+} in YAIO_3 to determine the dephasing times. These measurements were compared with the theory of Hu and Hartmann. The two-pulse echoes may be fit for the linewidth $\Delta\omega_{1/2} = 7000 \text{ s}^{-1}$ and host-spin flip-flop rate $W = 2100 \text{ s}^{-1}$. The linewidth parameter

$\Delta\omega_{1/2}$ is much smaller than that obtained from the theory and the measured inhomogeneous width for Pr^{3+} in YAIO_3 . The three-pulse echo data was fit by the Hu-Hartmann model using $W = 12 \text{ s}^{-1}$, $T_1 = 0.25 \text{ s}$, and $\Delta\omega_{1/2} = 100\,000 - 1.14/\tau \text{ s}^{-1}$. The apparent discrepancy between the two-pulse and the three-pulse fits is attributed to fluctuations caused by different host nuclei. For $\tau \geq T_2$, the bulk Al cause the dephasing. They are largely ineffective in dephasing for $\tau \ll T_2$, producing only a rapid small-amplitude change in the stimulated echo. For $\tau \ll T_2$, the frozen-core Al produce a much larger effective field which fluctuates at a much slower rate. Measurements of the relaxation of Al nuclear spins are needed to determine if the rates determined in this paper match the Al dynamics.²²

ACKNOWLEDGMENTS

I thank A. Szabo for many discussions in the course of this study and J. Froemel for technical assistance.

-
- ¹R. M. Macfarlane and R. M. Shelby, in *Spectroscopy of Solids Containing Rare Earth Ions*, edited by A. A. Kaplyanskii and R. M. Macfarlane (North-Holland, New York, 1987); K. P. Dinse, *J. Mol. Struct.* **192**, 287 (1990).
²S. Kroll, E. Y. Xu, M. Kim, M. Mitsunaga, and R. Kachru, *Phys. Rev. B* **41**, 11 568 (1990).
³A. A. Kaminskii (unpublished).
⁴R. M. Macfarlane, R. M. Shelby, and R. L. Shoemaker, *Phys. Rev. Lett.* **43**, 1726 (1979).
⁵P. Hu and S. R. Hartmann, *Phys. Rev. B* **9**, 1 (1974).
⁶J. Mlynek, N. C. Wong, R. G. DeVoe, and R. G. Brewer, *Phys. Rev. Lett.* **50**, 993 (1983).
⁷I. J. Lowe and M. Engelsberg, *Rev. Sci. Instrum.* **45**, 631 (1974).
⁸L. E. Erickson, *Phys. Rev. B* **42**, 3789 (1990).
⁹R. M. Shelby, C. S. Yannoni, and R. M. Macfarlane, *Phys. Rev. Lett.* **41**, 1739 (1978).
¹⁰N. C. Wong, E. S. Kintzer, J. Mlynek, R. G. DeVoe, and R. G. Brewer, *Phys. Rev. B* **28**, 4993 (1983).
¹¹L. E. Erickson, *Phys. Rev. B* **39**, 6342 (1989).
¹²L. E. Erickson, *Phys. Rev. B* **19**, 4412 (1979).
¹³L. Shen, *Phys. Rev.* **172**, 259 (1968).
¹⁴D. P. Burum, R. M. Macfarlane, R. M. Shelby, and L. Mueller, *Phys. Lett.* **91A**, 465 (1982); D. P. Burum, R. M. Macfarlane, and R. M. Shelby, *ibid.* **90A**, 483 (1982).
¹⁵The Hu-Hartmann model reduces to the J. R. Klauder and P. W. Anderson [*Phys. Rev.* **125**, 912 (1962)] two-pulse and

- stimulated echo model for short times and to the W. B. Mims [*Phys. Rev.* **168**, 370 (1968)] two-pulse model at long times. These theories use a continuous rather than a discrete lattice and therefore are approximate models. As a result, the $\Delta\omega_{1/2}$ constant obtained from the fits may differ from that derived from Eq. (2). In R. G. DeVoe, A. Wokaun, S. C. Rand, and R. G. Brewer, *Phys. Rev. B* **23**, 3125 (1981), the authors state that the Hu-Hartmann theory should not be applied to the optical measurement of Ref. 9 because the product of the duration of the measurement and the maximum frequency shift due to a spin flip is less than unity. The result is that the theory overestimates the frequency shift due to B -spin flips. [Klauder and Anderson, Eq. (3.14).] For the two-pulse and three-pulse measurements reported in this paper, this product is near unity.
¹⁶A. Abragam, *The Principles of Nuclear Magnetism* (Oxford University, New York, 1961), p. 258.
¹⁷B. R. Reddy and L. E. Erickson, *Phys. Rev. B* **27**, 5217 (1983).
¹⁸L. E. Erickson, *Phys. Rev. B* **24**, 5388 (1981).
¹⁹N. Bloembergen, *Physica* **15**, 386 (1949).
²⁰ $\Delta\omega_{1/2} = 66\,000 \text{ s}^{-1}$ is obtained from Eq. (2) if μ_A is replaced by $\hbar\gamma_A$. This formula would seem to apply only to the frozen-core broadening when such exists.
²¹Y. C. Chen, K. Chiang, and S. R. Hartmann, *Opt. Commun.* **29**, 181 (1979).
²²A. Szabo, T. Muramoto, and R. Kaarli, *Phys. Rev. B* **42**, 7769 (1990).